Viscoelastic Properties of an Epoxy Resin during Cure

DANIEL J. O'BRIEN[1]
Department of Mechanical and Industrial Engineering
University of Illinois at Urbana-Champaign
Urbana, IL 61801

PATRICK T. MATHER
Institute of Materials Science
University of Connecticut
Storrs, CT 06269

SCOTT R. WHITE
Department of Aeronautical and Astronautical Engineering
University of Illinois at Urbana-Champaign
Urbana, IL 61801

ABSTRACT: The cure dependent relaxation modulus of an epoxy resin was investigated over the entire range of cure extent. Parallel plate rheometry was used to measure the material behavior below the gel point of the epoxy network. Creep testing in three-point bend was used for specimens cured past gelation. All data were converted to the stress relaxation modulus for comparison of the material behavior among the various cure states and between the two experimental techniques. The data were used to develop a practical model for predicting the cure dependence of the relaxation modulus throughout cure under varying processing conditions.

INTRODUCTION

WARPAGE DUE TO processing induced residual stresses has long been recognized as a major obstacle to the efficient and cost-effective manufacture of composite parts. Recent research has demonstrated that careful selection of processing parameters can dramatically reduce warpage [1–5] suggesting that process modeling can be a powerful tool for determining optimal cure cycles. However, modeling residual stresses and warpage in composites is particularly difficult for

[1]Author to whom correspondence should be addressed. E-mail: djobrien@uiuc.edu

1530-793X/01/10 0883–22 $10.00/0 DOI: 10.1106/HLYM-5CM7-BP9N-L1Y1

several reasons. First, heat generation due to the crosslinking reaction as well as thermal asymmetry can result in uneven curing of the part. Second, epoxy resins can shrink by as much as 6% during cure. Finally, the matrix constitutive behavior is highly temperature dependent and spans the entire range of liquid to solid during processing. The present work addresses the last of these issues with experimental and analytical viscoelastic characterization of an epoxy resin throughout the entire cure process.

There has been limited work in the literature on the development of viscoelastic mechanical properties in curing thermosets. Some effort has focused on the development of relationships between viscoelastic properties and specific polymer characteristics, such as molecular weight, molecular weight distribution, and degree of chain branching [6]. White and Mather [7] investigated the effect of cure on viscoelastic properties using ultrasonic techniques. Dielectric spectroscopy has also been used in the characterization of curing polymers [8] by relating ionic mobility to dynamic viscosity.

Relaxation modulus data for epoxies cured according to various cure cycles were presented by Suzuki et al. [9]. However, the cure states of these samples were not determined. More recently, a detailed study of cure effects on the stress relaxation of a bisphenol A-derived epoxy was reported by Kim and White [10], including a model based on the Adams-Gibbs formulation for the volume relaxation in glasses. Also, an investigation of the cure dependence of the storage modulus for a commercial toughened epoxy was presented by Simon et al. [11] together with a model based on time-temperature-conversion for the cure effects on the viscoelastic response of thermosets. However, experimental data in each of these works were limited to cure states beyond the gel point. While it has been shown that knowledge of the material response in the postgelation regime is most important in modeling the development of residual stresses in composites [12], a complete understanding of the mechanisms that drive the development of material properties during cure cannot be achieved without knowledge of the material behavior throughout the entire cure cycle.

Due to obvious applications in molding processes, research on the mechanical response of thermosets below gelation has focused on measuring and modeling the development of resin velocity during cure [13]. Researchers in this area often measure the viscoelastic complex viscosity and relate it to the steady-shear viscosity using the Cox-Merz rule. Another common and convenient description of the mechanical behavior during cure is made through the time-temperature-transformation (TTT) diagram [14]. The TTT approach provides a graphical representation of the coupling between cure kinetics and the gelation and vitrification processes. Also, there has been work examining the viscoelastic response of thermosetting materials near the gel point [15,16].

Plazek and Chay [17] studied the evolution of viscoelastic properties in an epoxy resin both above and below gelation. Fully cured samples of a wide range of

crosslink densities were prepared by varying the ratio of monofunctional and tetrafunctional curing agents in a stoichiometric epoxide-curing agent mixture. This approach allowed the researchers to measure properties at fixed points in the network's development, even above the glass transition temperature (T_g). However, the network of each specimen is unique and a direct relation to the degree of cure is impossible. The degree of cure is a common manufacturing parameter often defined as,

$$\alpha = \frac{H(t)}{H_U} \tag{1}$$

where $H(t)$ is the heat released by the crosslinking reaction up to time t and H_U is the ultimate heat of reaction. To the authors' knowledge there has not been a complete study of the development of the viscoelastic properties of a thermoset for $0.0 \leq \alpha \leq 1.0$.

In this paper, the results of a detailed study of the viscoelastic response of a bisphenol F-derived epoxy over the entire range of cure are presented. Experiments were conducted in oscillatory shear with parallel plate rheometry at low cure states (pregelation), and creep under three-point bending for high cure states. The experimental data were used to develop a practical empirical model to predict the shear relaxation modulus during cure.

In the sections that follow the experimental procedure for both sets of experiments is presented first. Next, the procedure used for constructing creep compliance and dynamic moduli master curves from the creep and oscillatory data is presented along with the conversion of these material properties to the shear relaxation modulus. Following this, a cure-dependent stress relaxation material model is developed and correlated with the experimental data. Finally, the stress relaxation behavior during cure of this epoxy system is compared to that of the bisphenol A system previously reported by Kim and White [10].

EXPERIMENTAL PROCEDURE

Materials

The resin chosen for this study is EPON Resin 862 (Shell Chemical, Houston, TX), a difunctional epoxide formulated from the reaction of epichlorohydrin and bisphenol F [4]. The epoxide was cured with EPON Curing Agent W (Shell Chemical, Houston, TX), diethyltoluene diamine. The chemical structures of both materials are shown in Figure 1.

All specimens were manufactured using a stoichiometric combination of epoxide and amine (26.4/100 w/w epoxide/amine) and mixed using an automatic stirrer for 10 minutes followed by degassing for 30 minutes at approximately 25 in Hg.

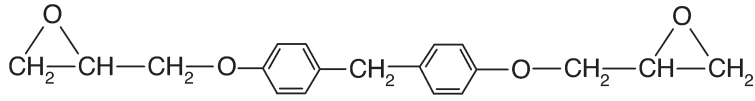

(a) epoxide

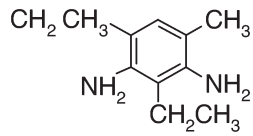

(b) amine

Figure 1. *Resin system investigated for this study: (a) EPON 862 (bisphenol F epoxide) and (b) EPON Curing Agent W (diethyltoluene diamine).*

Pregelation Characterization

Viscoelastic data at low cure states were obtained by oscillating the material is shear between parallel plates (8 mm diameter) using an RDA-II rheometer (Rheometric Scientific, Piscataway, NJ) with a tool geometry as shown schematically in Figure 2(a). Specimens were cured at 110°C for successively longer dwell times to achieve a range of cure states spanning from uncured to gelled. Sample preparation was carried out by preheating the test cell to 110°C and injecting a

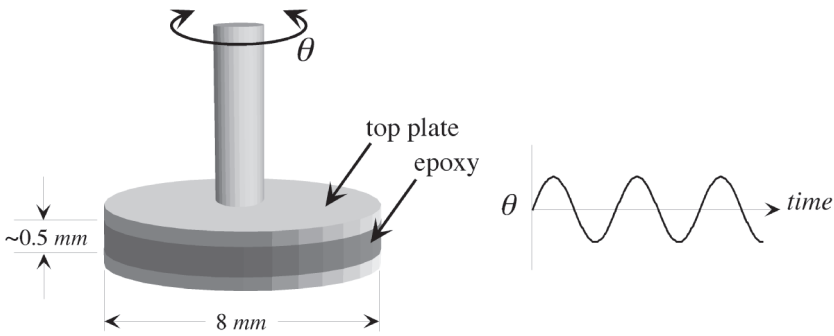

(a) parallel plate rheometry

Figure 2. *Experimental setups used in this study: (a) oscillatory shear between parallel plates and (b) creep under three-point bending.*

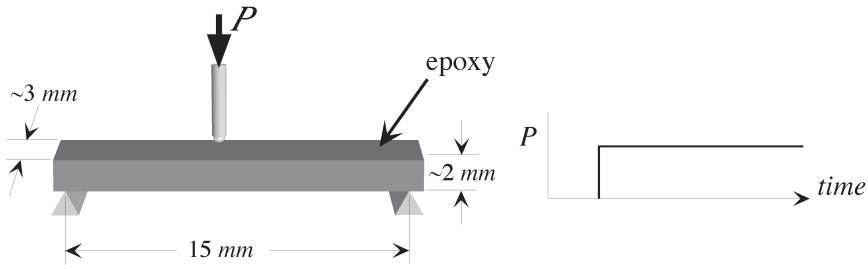

(b) 3-pt bend creep

Figure 2 (continued). *Experimental setups used in this study: (a) oscillatory shear between parallel plates and (b) creep under three-point bending.*

small amount of resin between the plates. After allowing the specimen to cure for a specified amount of time, the gap between the plates was set to approximately 0.5 mm and the specimen was dressed with a spatula so that the edge was flush with the edge of the plates. Then, residual heat of reaction, H_R, was measured by taking a small sample from the dressed material and placing it in a differential scanning calorimeter (DSC) (Rheometric Scientific, Piscataway, NJ) and performing an isothermal scan at 150°C. The degree of cure of the specimen is found by comparing the residual heat of reaction to the ultimate heat of reaction (399 ± 14.4 J/g [18])

$$\alpha = 1 - \frac{H_R}{H_U} \tag{2}$$

After curing, the rheometer was cooled to a temperature 10 to 50°C below the sample's glass transition. Next, a strain sweep was performed at 30 rad/s to determine the regime where the material exhibits linear behavior. Once an appropriate strain was determined, the complex moduli were measured by sweeping the frequency from 100 to 0.1 rad/s. The temperature was then raised 5 to 15°C and the procedure was repeated to obtain the material behavior spanning a range of temperatures. Cure advancement of samples at test conditions was negligible as confirmed by DSC analysis.

Postgelation Characterization

During manufacture and curing of the rheometer specimens it was found that cure shrinkage led to specimens of diameter significantly smaller than the installed plates. After cure, the gap beween the plates was adjusted so that the material fully

covered the surfaces and any excess material (squeezed out) was dressed with a spatula. While this technique worked well for specimens in the pre-gel state, postgelation specimens could not be adjusted after cure. Although there is a need to develop a specimen geometry that allows for cure shrinkage maintaining consistent boundary conditions, in this study we chose to use three-point bending to investigate the postgelation material behavior.

Three sets of specimens at different cure states were manufactured for three-point bend creep tests. After mixing, the resin was poured into a silicon rubber mold, degassed, and cured in a convection oven (Fisher Scientific, Pittsburgh, PA). After debonding, the specimens were sanded to the appropriate thickness using a polisher (Buehler, Lake Bluff, IL) and cut into small beams (nominally 15 mm × 3 mm × 2 mm) using a diamond saw (Buehler, Lake Bluff, IL). The residual heat of reaction was determined by isothermal DSC scans at 150°C of a piece of the specimen immediately before creep testing. Table 1 shows the cure cycles and resulting cure states of each specimen. The fully cured specimens were cured at 177°C, well above the material's ultimate T_g of 150°C. Unfortunately, all specimens could not be cured at this temperature because the reaction rate is too fast to ensure uniformity of cure state for partially cured specimens. Instead, specimens were cured at a temperature well above their ultimate $T_g(\alpha)$, but with a reaction rate slow enough so that small deviations in cure temperature or time would have a negligible effect on the ultimate degree of cure.

The creep tests were performed on a DMA 7e dynamic mechanical analyzer (Perkin-Elmer, Norwalk, CT) shown schematically in Figure 2(b). Specimens were tested in creep for 10–15 minutes at a load that resulted in no more than 1% strain. For the fully cured specimens, tests were performed at 17 temperatures ranging from 30 to 175°C, while for the partially cured specimens, the temperature was raised no higher than T_g to prevent additional curing. DSC scans of the speci-

Table 1. Specimen cure schedules and the resulting degree of cure.

Time (min.)	Temperature (°C)	α	Experiment
0	110	0.0	parallel plate
25	110	0.22	parallel plate
50	110	0.42	parallel plate
70	110	0.60	parallel plate
90	110	0.65	parallel plate
130	110	0.71	parallel plate
145	110	0.73	parallel plate
180	110	0.77	parallel plate
50	145	0.81	3-pt bend
120	145	0.90	3-pt bend
600	177	1.0	3-pt bend

mens after creep testing showed that no detectable cure advancement had occurred.

DATA ANALYSIS

Time-Temperature Superposition

The dynamic data and creep data at each cure state were shifted according to time-temperature superposition to obtain master curves with respect to reduced frequency, φ, and reduced time, ξ, defined by,

$$\xi = \int_0^t a_T(T)d\tau \tag{3}$$

$$\varphi = \int_0^\omega \frac{1}{a_T(T)}dv \tag{4}$$

where $a_T(T)$ is the shift function.

Figures 3 and 4 show typical master curves obtained from the oscillatory and creep experiments respectively. For all temperatures and cure states considered in this study the material exhibited time-temperature superposition with only horizontal shifting required to construct the master curves.

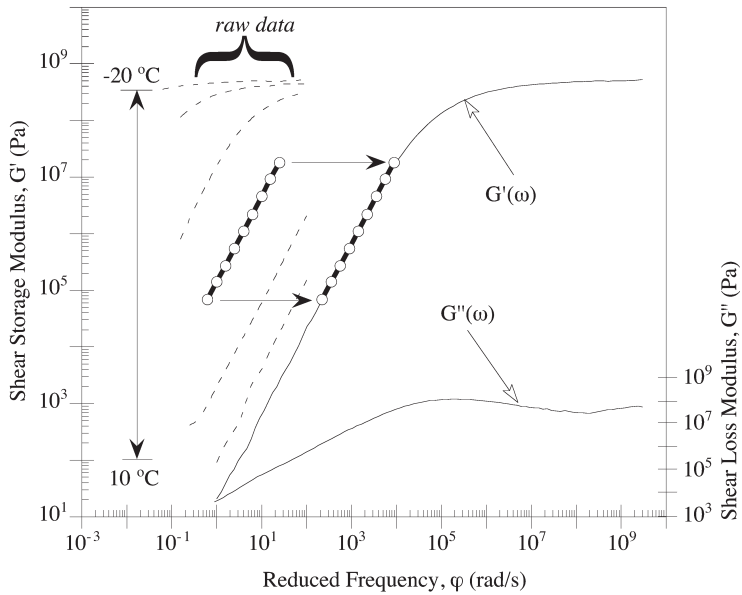

Figure 3. *Dynamic shear moduli master curve construction,* $\alpha = 0.22$, $T_{ref} = 10°C$.

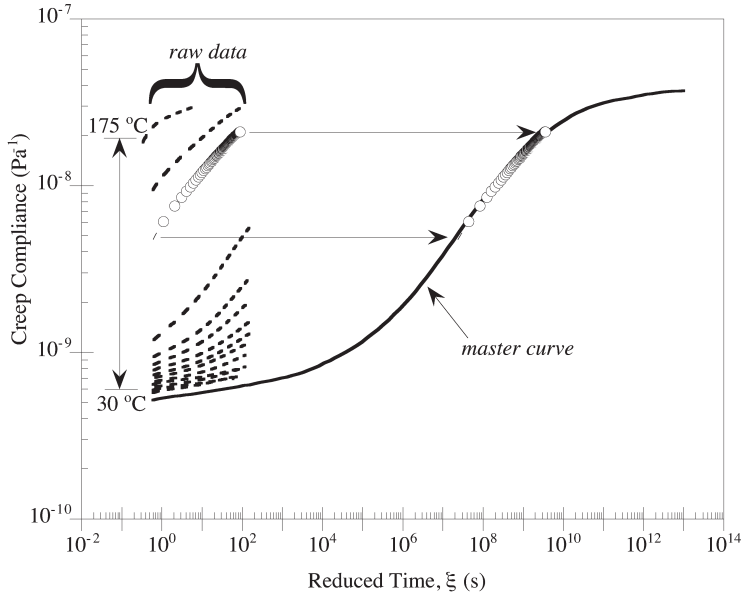

Figure 4. *Creep compliance master curve construction, α = 1.0, T_{ref} = 30°C.*

Figures 5 and 6 show the master curves obtained for all cure states for a reference temperature of 30°C. Unfortunately, reliable data were not obtained at 30°C for α = 0.0 and 0.22. Instead, the shift factor at 30°C was estimated from WLF fits to the available shift factor data above T_g for α = 0.0 and 0.22 specimens.

The shift factors used in constructing the master curves are given in Figure 7. The sample T_g, determined by DSC [18], provides a convenient temperature to compare the shift factor data among cure states. Past gelation the shift function shows a bi-linear temperature dependence over the temperature range investigated with a steep slope above T_g and a relatively shallow slope below T_g. Re-plotting the shift factors using the T_g as the reference temperature reveals the cure dependence of the two linear regions. This plot, shown in Figure 8, shows that below T_g the shift function increases in slope with advancing cure state while above T_g, the slope is nearly independent of cure state. Plazek and Chay [17] found similar behavior for the temperature dependence of the shift factor in the transition region.

Data Conversion

In order to compare the material behavior for different cure states and to model this behavior over the entire range of cure, the material response must be converted

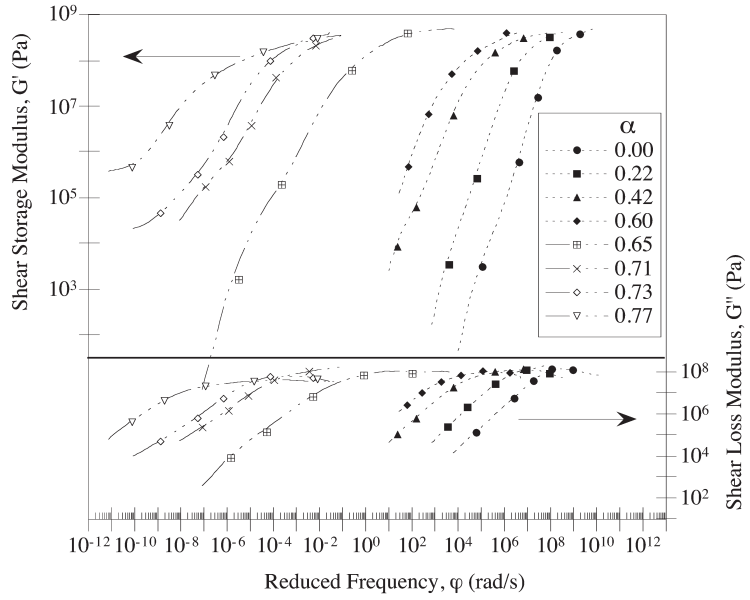

Figure 5. *Dynamic moduli master curves from oscillatory shear experiments,* T_{ref} *= 30°C.*

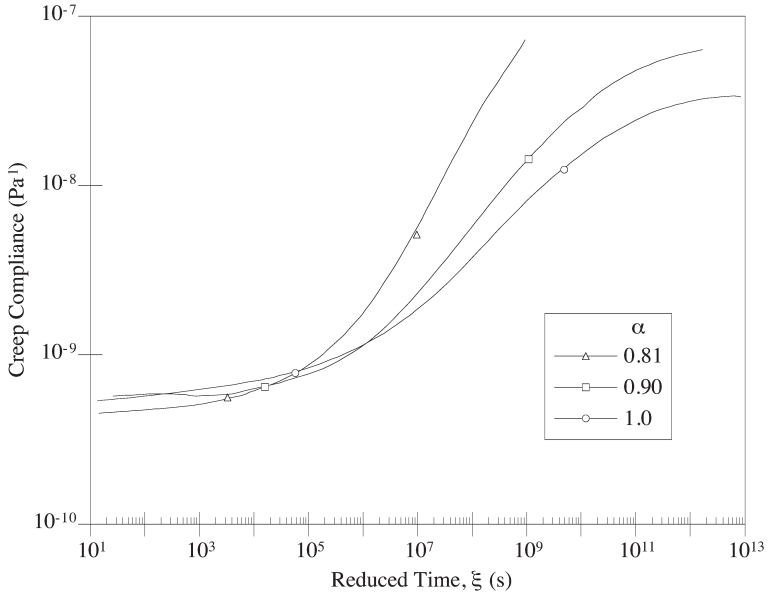

Figure 6. *Creep compliance master curves determined by creep testing of 3-point bend specimens,* T_{ref} *= 30°C.*

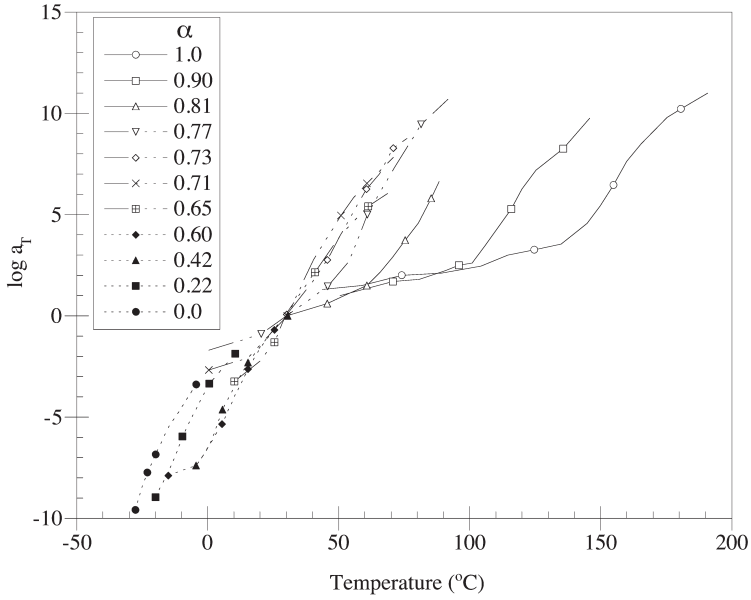

Figure 7. *Shift factors used in constructing master curves,* T_{ref} *= 30°C.*

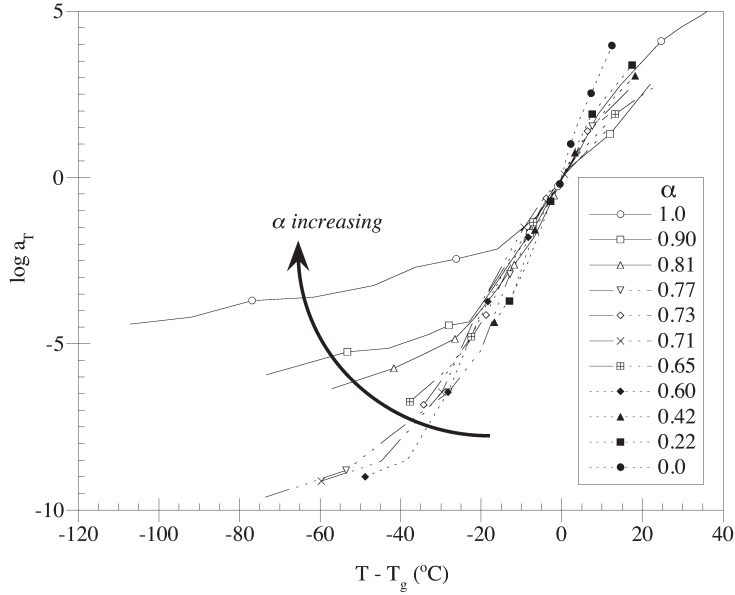

Figure 8. *Shift factors used in constructing master curves,* $T_{ref} = T_g$.

to a common form at each cure state. We chose to use the stress relaxation modulus as the material function, with the benefit of comparison to the behavior of the Hercules 3501-6 epoxy reported by Kim and White [10].

DYNAMIC MODULI

To convert the dynamic shear moduli obtained in the rheometry tests to the shear relaxation modulus, an approximate relation developed by Schwarzl and Struik [19] is used,

$$G(1.25t) = G'(\omega) - 0.5303G''(0.5282\omega) - 0.021G''(0.085\omega) + 0.042G''(6.37\omega) \quad (5)$$

where $\omega = 1/t$. This relation and others like it based on a method proposed by Ninomiya and Ferry [20] are derived by approximating the kernel of the transient behavior as a mixture of the kernels associated with the dynamic response. The maximum absolute error in using Equation (5) is $0.016G''(\omega)$. For the data presented here this corresponds to a relative error of no more than 10%.

CREEP COMPLIANCE

For linear viscoelastic materials, the creep compliance, $J(t)$, is related to the stress relaxation modulus, $E(t)$ through the following convolution integral [21],

$$\int_0^t E(\tau)J(t-\tau)d\tau = t \quad (6)$$

Alternatively, in the Laplace domain Equation (6) reduces to,

$$sJ(s) = \frac{1}{sE(s)} \quad (7)$$

where s is the Laplace parameter. Therefore, creep data can be fit in the time domain to a function that has a simple Laplace transform and then, through the use of Equation (7), the relaxation modulus in the Laplace domain can be easily determined. To obtain the relaxation modulus in the time domain, the inverse Laplace transform of $E(s)$ is found. If analytical inversion is difficult or impossible, then $E(s)$ can be fit (in the Laplace domain) to a functional form that is more easily inverted.

In this paper, the creep compliance data of the resin are fit to a generalized Voigt model given by [21],

$$J(t) = J_0 + \sum_{i=1}^{N} J_i \left[1 - \exp\left(\frac{-t}{\lambda_i} \right) \right] \tag{8}$$

where J_0 is the initial compliance, λ_i are retardation times, and J_i are the compliances associated with each term in the series.

The fitting was accomplished using the Levenberg-Marquardt non-linear curve fitting algorithm [22]. Equation (8) is easily transformed to the Laplace domain and the relaxation modulus in the Laplace domain is then found with Equation (7). Finally, the inverse Laplace transform of the resulting expression is determined by fitting (in the Laplace domain) to a Prony series given by,

$$E(s) = \frac{E_0}{s} + \sum_{i=1}^{N} \frac{E_i \tau_i}{1 + s\tau_i} \tag{9}$$

where E_0 is the equilibrium modulus, τ_i are relaxation times, and E_i are the moduli associated with each term in the series. Performing an inverse Laplace transform of Equation (9) gives the relaxation modulus in the time domain,

$$E(t) = E_\infty + \sum_{i=1}^{N} E_i \exp\left(\frac{-t}{\tau_i} \right) \tag{10}$$

where E_∞ is the equilibrium modulus.

Since the rheometry data are in terms of the shear modulus, it is necessary to relate the tensile relaxation modulus in Equation (10) to the shear relaxation modulus. Here the standard isotropy condition is assumed,

$$G(t) = \frac{E(t)}{2(1 + \nu)} \tag{11}$$

assuming a constant Poisson's ratio of $\nu = 0.35$. Though ν is expected to relax to ~0.5 as the material approaches the rubbery plateau, it was found that the effect on $G(t)$ is relatively minor.

Cure Dependent Relaxation Modulus

With all data converted to a common viscoelastic function, the material behavior can be compared over the entire range of cure. Figure 9 shows the shear relaxation modulus for all cure states considered. Generally, the figure shows the relaxation modulus developing in a self-similar manner over the entire range of cure and between the two experiment types. However, there is a slight inconsistency in the shape of the relaxation modulus at $\alpha = 0.77$ and $\alpha = 0.73$. Even though not evi-

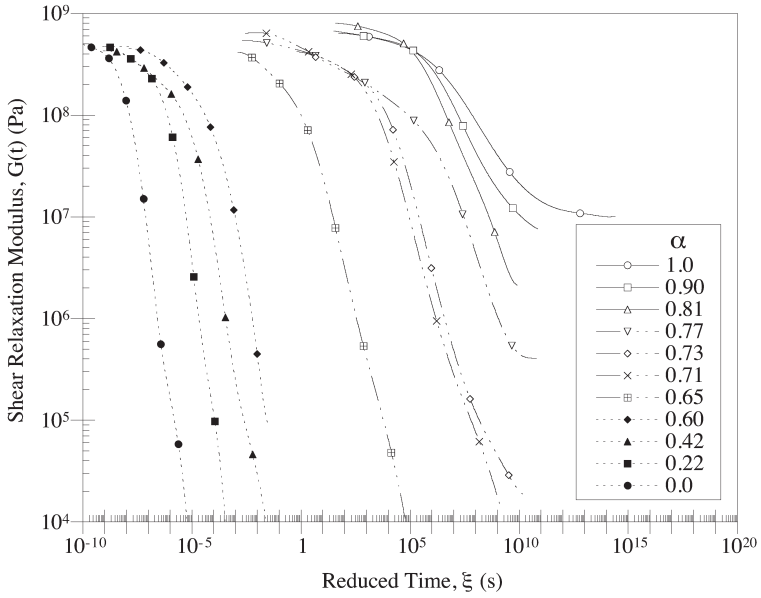

Figure 9. *Shear relaxation modulus of EPON 862/W over the entire range of cure,* T_{ref} *= 30°C.*

dent from DSC experiments, this inconsistency is likely due to inaccuracy in measurement of the cure state or further curing that occurred during the experiment and the proximity of these specimens to the gel point ($\alpha \approx 0.71$ [18]) where a very small change in cure state can have a significant effect on material properties.

Overall, the results indicated that small changes in the cure state have a profound effect on relaxation, especially near gelation. At cure states up to $\alpha = 0.60$, there is relatively little change in the relaxation behavior, which shifts from about 10^{-5} s (uncured) to about 10^{-2} s ($\alpha = 0.60$). However, as the material nears gelation the relaxation slows significantly. The relaxation modulus shifts approximately 5 decades along the log(time) axis between $\alpha = 0.60$ and $\alpha = 0.65$. Additionally, the character of the relaxation curve changes dramatically and shows strong chemorheologically complex behavior. Through gelation there is a noticeable broadening of the relaxation spectrum as the molecular weight (and presumably, the degree of branching) increases. The terminal region initially decreases in slope and then gives way to a rubbery plateau of about 10^5 Pa for $\alpha = 0.77$. The equilibrium modulus continues to increase past gelation to its final value of about 10^7 Pa. It is also worth noting that the initial modulus of the material is relatively insensitive to the cure state. This expected behavior was also observed by Kim and White [10] for Hercules 3501-6 epoxy resin as well as Plazek and Chay [17] for EPON 1001F epoxy.

Relaxation Spectrum

If the index N in Equation (10) is increased without bound, the relaxation modulus can be written in terms of the following integral equation [10],

$$G(t) = G_\infty + \int_{-\infty}^{\infty} H(t) \exp\left(\frac{-t}{\tau}\right) d(\ln \tau) \tag{12}$$

where $H(t)$ is the relaxation spectrum. Thus, the master curves in Figure 9 can be modeled using Equation (12) to obtain the relaxation spectra. However, it is common to use Alfrey's approximation [21] to accomplish this. Accordingly, a first-order approximation of the spectral response is used where,

$$H(t) \approx -\frac{dG(t)}{d \ln t} \tag{13}$$

Figure 10 shows the relaxation spectra for four of the cure states in Figure 9. The relaxation spectra provide additional insight into the effects of cure on material behavior. First, the amplitude of the primary relaxation peak shows a general decrease in magnitude as cure advances. This decrease in magnitude is accompa-

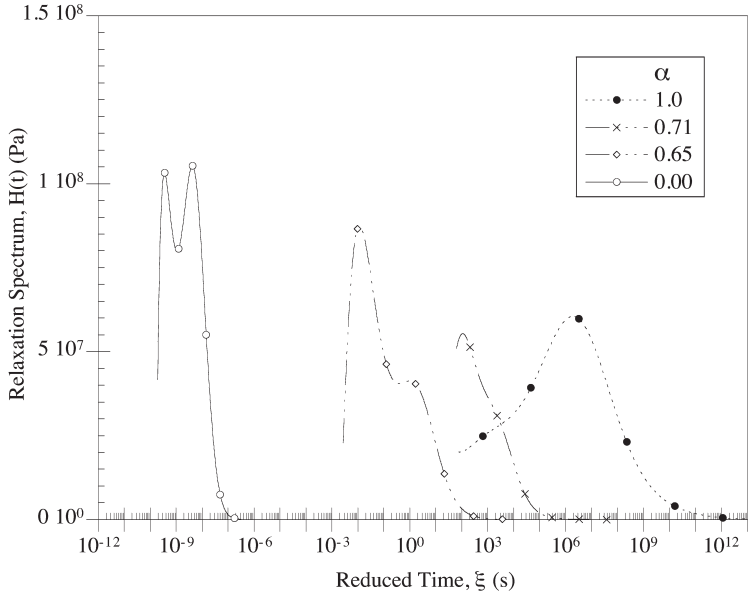

Figure 10. *Relaxation spectrum of EPON 862/W over the entire range of cure,* T_{ref} *= 30°C.*

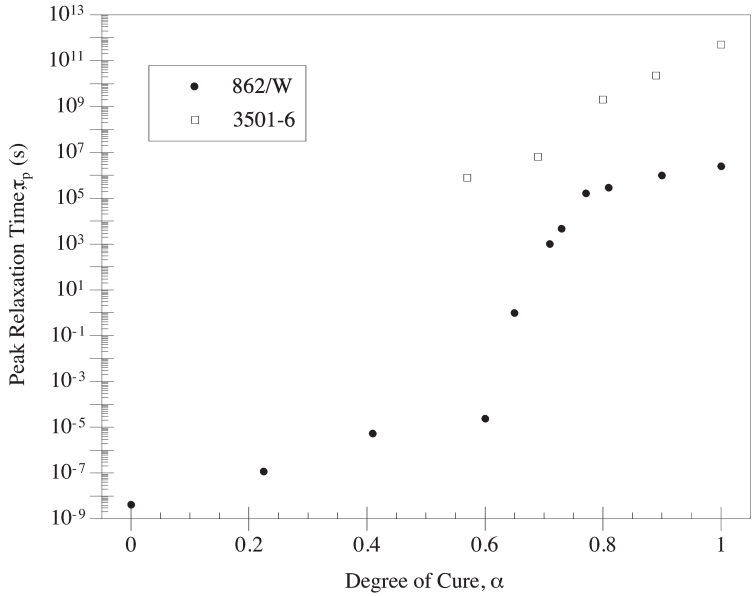

Figure 11. *Cure dependence of the peak relaxation time for EPON 862/W and Hercules 3501-6 [10].*

nied by a broadening of the spectral response from about 5 to 13 decades of time from uncured to fully cured states. The increase in breadth, estimated here by extrapolating the measured data to zero at either end of the spectrum, is indicative of the incorporation of more "modes" of relaxation as the network structure of the resin develops. Additonally, the spectrum indicates a possible crossover between dominant modes of relaxation near gelation when one of two peaks begins to dominate the relaxation spectrum.

Perhaps the most distinct piece of information that can be gained from the relaxation spectrum is the characteristic relaxation time, taken as the peak in the spectral response. Figure 11 shows the cure dependence of the peak relaxation time over the entire range of cure. There is little change in peak relaxation until after $\alpha \approx 0.60$ at which point a rapid increase commences through gelation. Interestingly, after gelation there is little change in the peak relaxation time as it changes by less than a decade from $\alpha = 0.80$ to 1.0. However, in that range of cure the material properties continue to evolve and the breadth of the relaxation spectrum increases by at least 5 decades of time.

MATERIAL MODELING

Stress relaxation data are often modeled with the stretched exponential or

Kohlrausch-Williams-Watts function as [23],

$$G(t) = G_u \exp\left[-\left(\frac{t}{\tau_p}\right)^{\beta}\right] \tag{14}$$

where G_u is the unrelaxed modulus, τ_p is the relaxation time, and β is a material parameter. However, Kim and White [10] found that it was not possible to accurately capture epoxy behavior over a sufficiently long time scale with a single value of β. Instead, they modeled the relaxation modulus of an epoxy resin with a series of exponentials (Prony series). The use of a Prony series is attractive for several reasons. First, it is flexible enough to capture a wide range of material behavior. Second, the terms in the model have physical significance, indicating which modes dominate during relaxation. Finally, the functional form of the model is amenable to numerical simulation of viscoelastic finite element algorithms utilizing recursive solution techniques [24].

The Prony series model is used here with the assumption that each term is cure dependent, i.e.,

$$G(t,\alpha) = G_\infty(\alpha) + \sum_{i=1}^{N} G_i(\alpha)\exp\left(\frac{-t}{\tau_i(\alpha)}\right) \tag{15}$$

where G_∞ is the equilibrium modulus and τ_i are relaxation times with associated amplitudes, G_i.

This approach assumes that one can identify a particular term in the Prony series at a given cure state and determine how that term develops as the material cures. However, simply fitting the data at each cure state to an N-term Prony series does not indicate how specific terms in the series relate to one another from one cure state to the next. Therefore, a reference time must be established for each cure state. The relaxaton times can then be fixed about this reference time and a Prony series can be fit to the data at each cure state. Subsequently, the cure dependence of each term in the Prony series can be determined.

The peak relaxation time as shown in Figure 11 was chosen as the reference time for modeling purposes in the present work. Figure 12 shows the relaxation modulus after shifting the data along the log(time) axis so that all peaks coincide at 10^0 seconds. After shifting to the reference peak, the data at each cure state were fit to an 11-term Prony series with G_i restricted to positive values and relaxation times fixed at each decade about τ_p, i.e,

$$\tau_i(\alpha) = \tau_p(\alpha) \cdot 10^i \tag{16}$$

where $i = -4$ to 6.

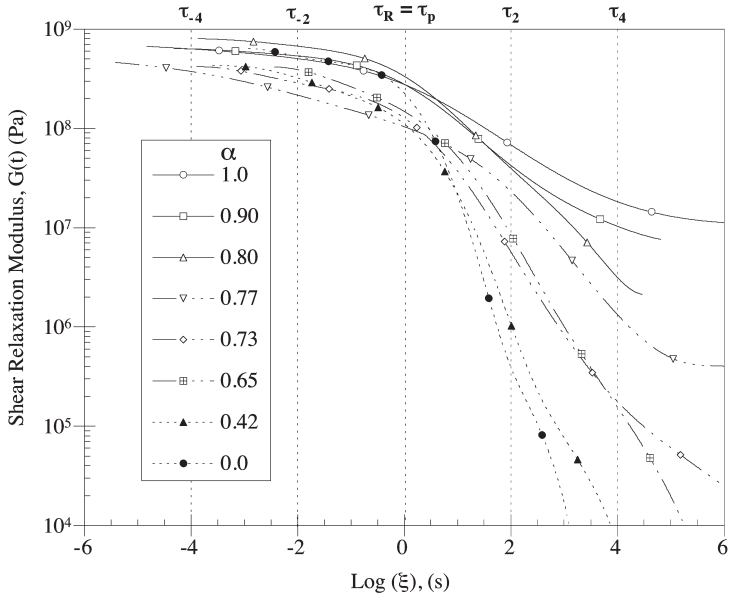

Figure 12. *Shear relaxation modulus at each cure state after shifting to the reference time,* τ_p.

Figure 13 shows the cure dependence of the Prony series coefficients. Below the peak relaxation time ($i \leq 0$) the Prony series coefficients are nearly independent of cure state. Above the peak relaxation time however, the coefficients show a very strong dependence on degree of cure rising in some cases by 3 orders of magnitude over the entire range of cure.

Linear fits are overlaid with the data in Figure 13. Since there is no strong cure dependence of the slope of the Prony series coefficients for $i \leq 0$, G_i is set constant for these terms. The parameters of the linear fits obtained for EPON 862/W are given in Table 2.

For the cure dependence of the equilbrium modulus we chose the empirical relation,

$$\log G_\infty = C + \frac{D}{1 + \exp\left(\dfrac{\alpha^* - \alpha}{F}\right)} \tag{17}$$

where C, D, and F are fitting parameters and α^* is the gel point. The parameters in Equation (17) were determined from the measured equilibrium moduli of $\alpha = 1.0$ and 0.77 and estimated values for the other cure states above gelation. Below gelation, the equilibrium modulus is arbitrarily assumed to be 0.1 Pa based on rhe-

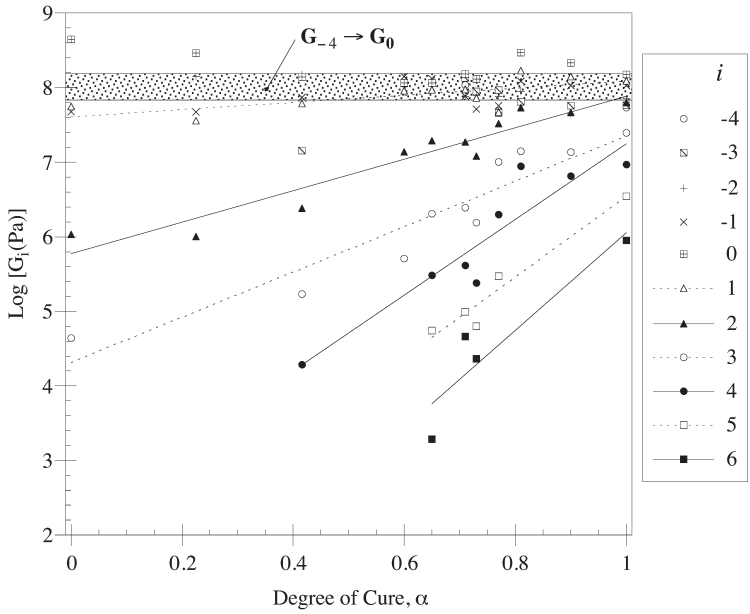

Figure 13. *Cure dependence of the Prony series coefficients.*

ometer measurements of the storage modulus during isothermal curing at 150°C and 30 rad/s. Although the equilibrium modulus is difficult to measure below gelation, the assumed value is so low that its influence on residual stress predictions is negligible. For these assumptions, $C = -0.93$ log(Pa), $D = 7.87$ log(Pa), $F = 0.046$, and $\alpha^* = 0.71$ for EPON 862/W.

Table 2. Parameters of the linear fits for the Prony series coefficients where log $G_i = A_i + B_i\alpha$.

i	*A* (log Pa)	*B* (log Pa)
–4	7.96	0
–3	7.66	0
–2	7.98	0
–1	7.47	0
0	8.2	0
1	7.63	0.52
2	5.78	2.12
3	4.3	3.03
4	2.17	5.08
5	1.14	5.4
6	–0.49	6.55

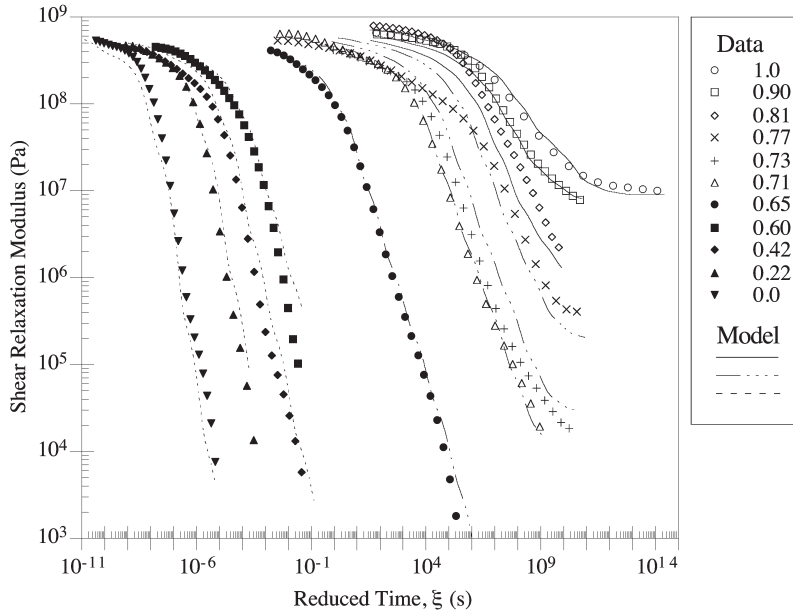

Figure 14. *Correlation between the experimental data and the cure dependent model proposed in Equation (15).*

With these fits and the peak relaxation times in Figure 11, the model in Equation (15) is overlaid with experimental data in Figure 14. The correlation between the model and experimental data is excellent for the entire range of cure. Table 3 lists all material parameters used in Equation (15) for EPON 862/W.

Table 3. Peak relaxation times used with Equations (15) and (16).

α	log τ_p (s)	τ_p (s)
0.0	–7.01	$9.76 * 10^{-8}$
0.22	–6.60	$2.53 * 10^{-7}$
0.42	–5.49	$3.27 * 10^{-6}$
0.60	–4.30	$5.03 * 10^{-5}$
0.65	–0.30	$5.06 * 10^{-1}$
0.71	2.55	$3.51 * 10^{2}$
0.73	4.19	$1.55 * 10^{4}$
0.77	4.82	$6.56 * 10^{4}$
0.81	5.44	$2.78 * 10^{5}$
0.90	5.99	$9.82 * 10^{5}$
1.0	6.38	$2.42 * 10^{6}$

COMPARISON TO 3501-6

In this section, the stress relaxation behavior of EPON 862/W is compared to that of Hercules 3501-6 epoxy as reported by Kim and White [10]. In order to compare the shapes of the relaxation spectra, the spectra are normalized by the magnitude of the relaxation peak of the fully cured material, $H(\tau)_{\alpha=1.0}$. Also, since T_g of 3501-6 is approximately 35°C higher than that of 862/W, the spectra are compared with respect to a reference time fixed at the peak relaxation time of each material.

The relaxation spectra of the fully cured materials are compared in Figure 15(a). With respect to the reference time and normalization, the relaxation behavior of each system is quite similar in both shape and breadth. However, considering the behavior at lower cure states as shown in Figure 15(b) for $\alpha \approx 0.9$ and Figure 15(c) for $\alpha = 0.8$, it is evident that the behavior of these two systems is quite different. For $\alpha \approx 0.80$ and 0.90, 3501-6 shows unimodal relaxation compared to the bimodal behavior of 862/W. Also, the shape of the relaxation spectrum of 862/W changes dramatically even above gelation with the breadth increasing by about 5 decades of time from $\alpha = 0.8$ to 1.0. Conversely, the character of the spectrum for 3501-6 changes very little over the same range of cure. Yet, even though the peak relaxation time of 862/W changes very little from $\alpha = 0.8$–1.0, 3501-6 shows a dramatic (10^3 s) rise over the same range of cure as shown in Figure 11.

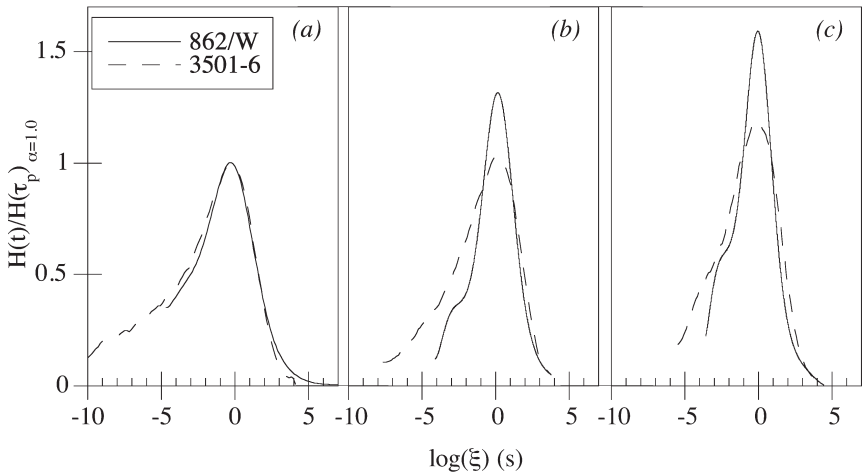

Figure 15. *Relaxation spectra normalized by* $H(\tau_p)_{\alpha=1.0}$ *for EPON 862/W and Hercules 3501-6 [10] at various cure states: (a)* $\alpha = 1.0$, *(b)* $\alpha \approx 0.90$, *(c)* $\alpha \approx 0.80$.

CONCLUSIONS

An experimental method for the viscoelastic characterization of a thermosetting resin over the entire range of cure was demonstrated using parallel plate rheometry and 3-point bend creep. Pregelation properties were measured with the rheometer, while above gelation, three-point bending was used. It was shown that for EPON 862/W the elastic response was nearly independent of cure state. However, the equilibrium modulus increased from undetectable levels to about 10^7 Pa at full cure. Over the entire range of cure, the peak relaxation time showed an increase of more than 12 orders of magnitude, predominantly near the gel point. A complex relaxation behavior was evidenced by a broad bimodal relaxation spectrum.

An empirical model for the shear relaxation modulus was developed by using the peak relaxation time as a reference time for determining the cure dependence of model parameters. The resulting model showed excellent correlation to experimental data over the entire range of cure states.

ACKNOWLEDGEMENTS

The authors would like to thank the National Science Foundation for support of this work through grant number NSF DMI-10382, Delsie Durham program manager. Additional support has been provided by the National Aeronautics and Space Administration, Johnson Space Center through grant number NASA NGT 9-33, Jeremy Jacobs JSC advisor. Also, Professors Philippe Geubelle and Charles L. Tucker III have provided technical advice throughout this research.

REFERENCES

1. S. R. White and H. T. Hahn. Process Modeling of Composite Materials: Residual Stress Development during Cure. Part II. Experimental Validation. *Journal of Composite Materials,* 26(16):2423–2453, 1992.
2. Q. Zhu, M. Li, P. H. Geubelle and C. L. Tucker III. Dimensional Accuracy of Thermoset Composites: Process Simulation. To appear in *Journal of Composite Materials,* 2001.
3. M. Li, Q. Zhu, P. H. Geubelle and C. L. Tucker, III. Optimal Curing for Thermoset Matrix Composites: Thermochemical Considerations. To appear in *Polymer Composites,* 22(1), 2001.
4. H. W. Wiersma, L. J. Peters and R. Akkerman. Prediction of Springforward in Continuous-Fibre/Polymer L-Shaped Parts. *Composites Part A,* 29A:1333–1342, 1998.
5. D. W. Radford. Cure Shrinkage Induced Warpage in Flat Uni-Axial Composites. *Journal of Composite Technology and Research,* 15(4):290–296, 1993.
6. S. A. Bidstrup and C. W. Macosko. Chemorheology Relations for Epoxy-Amine Crosslinking. *Journal of Polymer Science: Part B: Polymer Physics,* 28:691–709, 1990.
7. S. R. White and P. T. Mather. A Comparison of Ultrasonic and Thermal Cure Monitoring of an Epoxy Resin. *Composite Polymers,* 4(6):403–422, 1992.
8. J. O. Simpson and S. A. Bidstrup. Rheological and Dielectric Changes during Epoxy-Amine Cure. *Journal of Polymer Science: Part B: Polymer Physics,* 33:55–62, 1995.

9. K. Suzuki, Y. Miyano and T. Kunio. Change of Viscoelastic Properties of Epoxy Resin in the Curing Process. *Journal of Applied Polymer Science,* 21:3367–3379, 1977.
10. Y. K. Kim and S. R. White. Stress Relaxation Behavior of 3501-6 Epoxy Resin during Cure. *Polymer Engineering and Science,* 36(23):2852–2862, 1996.
11. S. L. Simon, G. B. McKenna and O. Sindt. A Thermo-Viscoelastic Model for the Mechanical Properties of an Epoxy during Cure. *Journal of Applied Polymer Science,* 76(4):495–508, 2000.
12. Y. K. Kim. *Process-Induced Viscoelastic Residual Stress Analysis of Graphite-Epoxy Composite Structures.* PhD thesis, University of Illinois at Urbana-Champaign, Department of Aeronautical and Astronautical Engineering, October 1995.
13. P. J. Halley and M. E. McKay. Chemorheology of Thermosets—An Overview. *Polymer Engineering and Science,* 36(5):593–609, 1996.
14. M. T. Aronhime and J. K. Gillham. Time-Temperature Transformation (TTT) Cure Diagram of Thermosetting Polymeric Systems, in *Epoxy Resins and Composites III.* Karel Dusek, editor, pp. 83–113. Springer-Verlag, 1986.
15. R. H. Valentine, J. D. Ferry, T. Homma and K. Ninomiya. Viscoelastic Properties of Polybutadienes—Linear and Lightly Crosslinked Near the Gel Point. *Journal of Polymer Science: Part A-2,* 6:479–492, 1968.
16. H. H. Winter and F. Chambon. Analysis of the Linear Viscoelasticity of a Crosslinking Polymer at the Gel Point. *Journal of Rheology,* 30(2):367–382, 1986.
17. D. J. Plazek and I.-C. Chay. The Evolution of the Viscoelastic Retardation Spectrum during the Development of an Epoxy Resin Network. *Journal of Polymer Science: Part B: Polymer Physics,* 29:17–29, 1991.
18. D. J. O'Brien and S. R. White. Cure Kinetics, Glass Transition, and Gelation of EPON 862/W Epoxy. Submitted to *Polymer Engineering and Science,* 2001.
19. F. R. Schwarzl and L. C. E. Struik. Analysis of Relaxation Measurements. *Advances in Molecular Relaxation Processes,* 1:201–255, 1967.
20. K. Ninomiya and J. D. Ferry. Some Approximated Equations Useful in the Phenomenological Treatment of Linear Viscoelastic Data. *Journal of Colloid Science,* 14:36–48, 1959.
21. J. D. Ferry. *Viscoelastic Properties of Polymers.* J. Wiley and Sons, New York, third edition, 1980.
22. W. H. Press, S. A. Teukolsky, W. T. Vetterling and B. P. Flannery. *Numerical Recipes in FORTRAN.* Cambridge University Press, Cambridge, second edition, 1992.
23. K. L. Ngai and D. J. Plazek. Identification of Different Modes of Molecular Motion in Polymers That Cause Thermorheological Complexity. *Rubber Chemistry and Technology,* 68:376–434, 1995.
24. S. R. White and Y. K. Kim. Process-Induced Residual Stress Analysis of AS4/3501-6 Composite Material. *Mechanics of Composite Materials and Structures,* 5:153–186, 1998.